

ITC 3/51 Information Technology and Control Vol. 51 / No. 3 / 2022 pp. 515-530 DOI 10.5755/j01.itc.51.3.30795	Weber Global Statistics Tri- Directional Pattern (WGSTriDP): A Texture Feature Descriptor for Image Retrieval	
	Received 2022/02/23	Accepted after revision 2022/08/10
	 http://dx.doi.org/10.5755/j01.itc.51.3.30795	

HOW TO CITE: Chelladurai, C. C., Vayanaperumal, R. (2022). Weber Global Statistics Tri- Directional Pattern (WGSTriDP): A Texture Feature Descriptor for Image Retrieval. *Information Technology and Control*, 51(3), 515-530. <http://dx.doi.org/10.5755/j01.itc.51.3.30795>

Weber Global Statistics Tri- Directional Pattern (WGSTriDP): A Texture Feature Descriptor for Image Retrieval

Callins Christiyana Chelladurai

Department of Computer Science and Engineering; Mangayarkarasi College of Engineering; Madurai, Tamilnadu, India; e-mail: callinschristiyana@gmail.com

Rajamani Vayanaperumal

Department of Electronics and Communication Engineering; Vel Tech Multi Tech Dr. Rangarajan Dr. Sakunthala Engineering College; Chennai, Tamilnadu, India; e-mail: rajavmani@gmail.com

Corresponding author: callinschristiyana@gmail.com

The texture is a high-flying feature in an image and has been extracted to represent the image for image retrieval applications. Many texture features are being offered for image retrieval. This paper proposes a local binary pattern-based texture feature called Weber Global Statistics Tri-Directional Pattern (WGSTriDP) to retrieve the images. This pattern combines the advantages of differential excitation components in the Weber Local Binary Pattern (WLBP), sign and magnitude components in the Local Tri- Directional Pattern (LTriDP), and global statistics. Differential Excitation (DE) and Global Statistics Tri- Directional Pattern (GSTriDP) are two components of WGSTriDP. The WGSTriDP gains the benefit of discrimination concerning human perception from differential excitation as well as incorporates global statistics into sign and magnitude components in the pattern derived from the local neighborhoods. The effectiveness of the pattern in image retrieval is experimented with in two benchmark databases, such as ORL (face database) and UIUC (texture database). According to the results of the experiments, WGSTriDP outperforms other local patterns in retrieving similar images from the database.

KEYWORDS: Weber Global Statistics Tri-Directional Pattern, Image Retrieval, Texture Feature, Local Patterns, Feature Extraction.

1. Introduction

Millions of digital images are being produced and shared due to the encroaching use of smart devices and the internet. It is necessary to search and retrieve the relevant images from the image collection, and image retrieval is an active research problem [16,40]. Image retrieval requires the user to input a query image and the system outputs similar images to the query from the image collection. The outdated methods of image retrieval exploit the methodologies of incorporating some captions or descriptions into the images so that retrieval can be accomplished with the help of them. But adding descriptions to every image in a large database is a time-consuming and expensive process. The automatic description or annotation of the images in the image database makes the retrieval process simple.

Content-Based Image Retrieval (CBIR) is a system that facilitates automatic image annotation. CBIR extracts the visual features from the query image and compares them with the visual features of the images placed in the collection [28]. The closest visual similarity images from the image collection are retrieved as similar images to the query. Low-level visual features such as color, texture, and shape [35] are extracted from the images to determine their visual similarity.

Color is one of the most important aspects of image representation. The human visual system discriminates between real-world objects based on color initially. Color Histogram [39], Dominant Color Descriptor [27], Color Coherence Vector [26], Color Correlogram [7], Block Truncation Coding [13], Color Moments [8], and other methods exist. The computational cost of deriving the features from the above-mentioned methods and their corresponding accuracy in retrieval applications is varied. Color features are rotation and translation invariant, but luminance invariant color features are challenging to achieve.

The image's shape [42] is defined as the image's characteristic surface configuration. The images are distinguished by their outline in shape based retrieval. The shape of the image is represented either by its boundary or its region. The outward boundary of the shape is used to represent the image in boundary

based shape representation. The image is described by the pixels along the image boundary. Region based shape representation uses the entire shape region and describes the considered region using the pixels present in that region. Since the segmentation is applied to describe the shape, the shape feature alone is not primarily used for image retrieval. Shape based features are combined with other low level features such as color and texture to represent the images for retrieval applications.

The texture is the intrinsic property of all surfaces that describes visual patterns, and it is also important to describe the features of different image collections available online. They are extracted from the images by structural and statistical methods. Structural methods are useful for describing artificial textures, whereas, statistical methods are simple and widely used to extract the texture features. Statistical methods apply quantitative measurements of intensity arrangements in a region. Gray Level Co-occurrence Matrix (GLCM) [6], Tamura features [33], Wavelet coefficients [17], Ridgelets and Curvelets [32], Gabor wavelet filter [18], Gray level histogram, edge histogram, and Local Binary Pattern (LBP) [24] are some of the more well-known statistical texture extraction methods.

The most prevalent and simple method among various texture representations is the Local Binary Pattern (LBP). LBP is illumination invariant besides its simplicity and computational efficiency. LBP is applied in medical image analysis, texture classification, face detection, and motion analysis by various researchers. Many local binary pattern variants are being developed for various image retrieval purposes. Due to the consideration of magnitude and sign patterns, Local Tri-directional Pattern (LTriDP) [38] and Local Neighborhood Intensity Pattern (LNIP) [1] were found to be superior features for textured image retrieval. But still, the question is how these patterns can be improved further so that the image retrieval system will bring the results closer to human discrimination. Our proposed effort aims to create a robust local binary pattern variant for image retrieval applications that is as close to human discrimination as possible.

This research article encompasses the literature survey of the image retrieval system with various texture

features for many applications under Section 2. The proposed methodology is given in Section 3. Section 4 shows the experimental results of the proposed work. Finally, the conclusion is provided in Section 5.

2. Literature Survey

Ojala et al. [25] presented a simple and powerful texture classification operator based on local binary patterns. They formed the rotation invariant local binary pattern by considering the different neighborhood sizes of 8-neighborhood, 16-neighborhood, and 24-neighborhood. The relationship between the center pixel and the surrounding pixels in the neighborhood is exploited for pattern formation. The experiment was conducted on Outex and Brodatz textures for texture classification. They proved that joint histograms formed by multi-resolution give the highest classification accuracy.

Tan et al. [34] offered Local Ternary Pattern (LTP) as the texture representation for the face recognition system. As an extension of LBP, ternary encoding is done in LTP. They showed that replacing LBP with LTP improved the recognition rate by about 5%.

The dominant local binary pattern for texture classification was described by Liao et al. [14]. The dominant local binary pattern uses 80% of the frequently occurring patterns in the conventional LBP. The dominant local binary pattern was applied in the Outex, Brodatz, Meastex, and CURET texture image databases. According to the authors, the dominant local binary pattern outperformed other preceding techniques in terms of classification accuracy under varied imaging conditions.

Murala et al. contributed Maximum Edge Binary patterns (LMEBP) [22], Directional Local Extrema Patterns (DLEP) [20] and Local Tetra Patterns (LTrP) [21] for CBIR applications. The three patterns, LMEBP, DLEP, and LTrP use the neighborhood relationship and extract maximum edges, directional edge information and $(n-1)^{\text{th}}$ order derivatives respectively, to form the feature vector of the image.

Zhang et al. [41] presented a Local Derivative Pattern (LDP) for face recognition. The local derivative pattern encodes the directional pattern features based on local derivative variations. The n^{th} order LDP is used

to encode the spatial relationship contained in the local region, whereas the LBP uses the local neighborhood for encoding. The authors conducted extensive experiments with LDP and LBP. They concluded that higher order LDP performs much better than LBP for face verification and identification problems under varying imaging conditions.

Guo et al. [5] contributed a Completed Local Binary Pattern (CLBP) operator for texture classification. CLBP integrates the sign component, magnitude component, and binary labeling of the center pixel in a neighborhood to represent the image. The sign component of CLBP represents the conventional LBP. The authors showed a substantial improvement in texture classification accuracy with the components of CLBP compared to the LBP algorithms.

Murala et al. [23] presented rotation invariant Local Ternary Co-occurrence Patterns (LTCoP) for MRI and CT image retrieval. The LTCoP encodes the co-occurrence of similar edges in a ternary fashion, which is determined by the gray values of neighborhood's center pixel and its surrounding neighbors in radius 1 and radius 2 distance. The ternary map is divided into binary maps for feature map construction. The authors used the LTCoP feature map to extract biomedical images and found that it was more effective than LBP, LTP, and LDP at retrieving the images.

Verma et al. [37] presented the Center Symmetric Local Binary Co-occurrence Pattern (CSLBCoP) for multipurpose image retrieval. CSLBCoP combines the features of Center Symmetric LBP (CSLBP) and GLCM. CSLBP gathers local information from the image. Gray Level Co-occurrence Matrix (GLCM) of the CSLBP pattern map perceives the co-occurrence of pixel pairs in different directions and distances. The GLCM of the pattern map provides mutual occurrence of patterns with more local information than the CSLBP map. The image retrieval algorithm was employed on texture, face, and medical databases. The results showed the superior performance of CSLBCoP as opposed to LBP, CSLBP, DLEP, LEPINV, and LEPSEG.

Verma et al. [36] have given a Local Neighborhood Difference Pattern (LNDP) for content-based image retrieval applications. It is a complementary technique to the local binary pattern. While LBP finds the relationship between the center pixel and the sur-

rounding pixels in the neighborhood, LNBP finds the mutual relationship among the surrounding neighbors. The image is represented by the combined feature vector of LBP and LNBP as they complete each other to furnish the local information. The feature was experimented with in texture and natural image databases to prove its efficacy. The experimental results demonstrated that the combined feature overtakes LBP, CSLBP, DLEP, LTrP, LEPINV, and LEPSEG in terms of retrieval accuracy.

Verma et al. [38] presented the Local Tri directional Pattern (LTriDP) for content based image retrieval. The intensity relationship of each surrounding pixel in a neighborhood is captured in three directions with three pixels. The center pixel and the two adjacent neighbors of each surrounding neighbor are utilized for the relationship. The sign and magnitude components are extracted with the effect of the relationship. The feature vector of the LTriDP is formed with the help of sign and magnitude patterns. The experiment was conducted in the Brodatz texture image database, the MIT VisTex database, and the AT&T face database. The retrieval results demonstrated LTriDP's superiority over other local pattern techniques.

The Local Neighborhood Intensity Pattern (LNIP) for content based image retrieval was developed by Banerjee et al. [1]. The feature vector for LNIP is computed, based on the sign and magnitude components of each surrounding pixel in a neighborhood. The surrounding pixels of a neighborhood are related to the center pixel and all the adjacent neighbors to it. The experiment was conducted in the Brodatz texture image database, the MIT VisTex database, the Salzburg texture database, and the AT&T face database. The authors concluded that LNIP outperforms other local methods in retrieval accuracy.

Chen et al. [3] introduced the Weber Local Descriptor (WLD) for texture classification and some other applications. The WLD feature is formed by differential excitation and orientation components. The differential excitation function is computed as the ratio of the relative intensity differences of a center pixel with its surrounding neighbors and the intensity of the center pixel. The gradient orientation of the current pixel is taken as the orientation component. The authors proved the effectiveness of WLD in texture classification as opposed to other state-of-the-art methods, including SIFT and LBP.

Liu et al. [15] presented the Weber Local Binary Pattern (WLBP) for the face recognition problem. WLBP has two components. They are differential excitation and LBP. The perception and local features are derived from differential excitation and LBP, respectively. The experiment was conducted on the Brodatz and KTH-TIPS2 texture databases. Even with diverse image obstacles such as facial expression, lighting, and noise, the results indicated that WLBP outperformed SIFT, LBP, WLD, and MLBP.

Sukhia et al. [30] demonstrated a multi-scale local ternary pattern for remote sensing image retrieval. They down sample the image into multiple scales and split them into patches to derive local ternary pattern (LTP) features. The final histogram representation is produced by Fisher vector coding followed by normalization. They conducted experiments on a land-use scene image dataset and a land-cover image dataset. The performance of the multi-scale local ternary pattern is compared with that of fusion similarity based reranking (FSR) and two-stage reranking (TSR) in terms of average precision and average retrieval time. They proved that multi-scale local ternary patterns surpassed multi-scale CLBP, FSR, and TSR.

Sukhia et al. [31] presented a content based histopathological image retrieval scheme based on multi-scale, multichannel decoded local ternary pattern features and VLAD coding. The method divides an image into multiple scales and employs a decoder-based local ternary pattern to generate upper and lower texture images in each level. A patch-based histogram is gained at each scale, which is followed by Vector of Linearly Aggregated Descriptors (VLAD) coding and power-law normalization. The experiments were conducted on the KIMIA Path960 dataset. The performance of the method is compared with multichannel decoded local binary patterns and local binary patterns. The experiments illustrated that the multi-scale, multichannel decoded local ternary pattern technique scored the highest precision and recall for the retrieval of 5, 10, 15, and 20 images over the multichannel decoded local binary pattern and local binary pattern.

Kanwal et al. [11] contributed the novel technique of combining image features with features generated by ResNet architecture. They proved that information carried by the image contents, such as spatial color, salient objects and texture, is further strengthened by the signatures produced by the ResNet architecture.

They proved that an image retrieval system with the integrated features gives outstanding results, even in the challenging datasets.

Kanwal et al. [10] presented an image retrieval system using deep learning techniques. Initially, they extracted the primitive image features, namely, Eigenvalues textured and convolutional Laplacian scaled object features with mapped colored channels from the image. The primitive images features are then fused with deep learning networks such as GoogLeNet, ResNet-50, VGG-19 to enhance the accuracy of the image retrieval over large image datasets. They conducted experiments on 10 benchmark datasets and showed the remarkable outcomes.

Ershad et al. [4] contributed an improved local ternary pattern to classify the bark texture images. The improved Local ternary pattern is coded with two local binary patterns, and then each binary pattern is classified into uniform and non-uniform patterns. The patterns are labeled with a degree of uniformity. The feature vector is formed based on the occurrence probability of the labels. The authors concluded that the improved local ternary pattern not only improves the classification accuracy but also provides noise-resistant and rotational invariant behaviors.

Kas et al. [12] designed multi-level directional cross binary patterns for texture classification. The pattern is handcrafted by encoding the informative directions from multiple radius neighborhoods. They proved that a multi-level directional cross binary pattern helps in identifying gray level variations that occur in different directions.

Multiple channels LBP [29] encodes the color image using inner and intra channel features, and the local features are extracted from three channels at once. The sign and magnitude components are extracted from color differences. Experimental results demonstrate that Multiple Channels LBP achieves good classification accuracy compared to most of the existing color texture features.

It is observed from the literature survey, that the local patterns are developed based on how they exploit the relationship between the center pixel and its surrounding neighbor pixels in a small neighborhood. Patterns that consider sign and magnitude components perform better as compared to those patterns that only consider sign components. The pattern that comprises the differential excitation followed by Weber's law recognizes human faces as compiled

with human perception. The inclusion of global statistics in an image makes the pattern robust to noise.

The three observations mentioned above prompted us to propose the pattern WGSTriDP, which derives texture from an image by combining differential excitation, a sign and magnitude patterns in a neighborhood, and global statistics.

The motivation of the proposed work is to develop the local pattern that complies with the human discrimination features to extract the texture features from the image for the applications of image retrieval. The following are the contributions to achieve the desired goal.

- 1 The local pattern is formed by deriving both the sign and magnitude components from the neighborhood relationship.
- 2 The differential excitation component is fused with the local pattern to incorporate human discrimination ability.
- 3 The global statistics is also combined with the local pattern, making the pattern more robust even in the presence of noise.

3. Proposed Framework

The proposed pattern WGSTriDP has two components. They are differential excitation component and GSTriDP. The relationship between the center pixel and the surrounding neighbors of the 3×3 neighborhood in an image is considered for differential excitation computation. The relationship between the nearest neighbors of the nearest neighbors of the surrounding pixels in a circular fashion and the center pixel is used for the GSTriDP pattern computation. The GSTriDP pattern is divided into two parts that deal with the relationships between local statistics in the 3×3 neighborhood and global statistics of an image.

3.1. Computation of Differential Excitation Component

A Differential Excitation pattern is computed for each pixel of an image. The 3×3 neighborhood is considered for each pixel to compute the differential excitation pattern. Figure 1 shows the 3×3 neighborhood of the pixel.

Figure 1
The 3×3 Neighborhood of a Pixel I_c

I_1	I_2	I_3
I_8	I_c	I_4
I_7	I_6	I_5

I_c in Figure 1 represents the intensity of the center pixel and I_1, I_2, \dots, I_8 represent the intensity of the surrounding neighbors. The differential excitation of the center pixel is calculated using Equation (1).

$$de(I_c) = \arctan \left(\frac{\sum_{i=1}^8 (I_i - I_c)}{I_c} \right) \quad (1)$$

$de(I_c)$ has a value between $[-\Pi/2, +\Pi/2]$. If the value is positive, it means the surrounding neighbors are lighter than the center pixel or else the surrounding pixels are darker than the center pixel. The histogram of differential excitation is formed once $de(I_c)$ is calculated for all the pixels of an image. To build the histogram of the differential excitation component, the range $[-\Pi/2, +\Pi/2]$ is divided into several bins. The constant K is used to divide the range into low perception and high perception intervals. The range $[-K: K]$ is called the low perception interval and $[-\Pi/2: -K]$ and $[K: \Pi/2]$ are called high perception intervals. The high perception intervals are further partitioned into several bins as they contain more information. The constant S is utilized for this partition. The value of 'S' is chosen as odd according to symmetry. The differential excitation values are quantified to the 'S' intervals and they are exploited to form a differential excitation histogram of an image. Equation (2) describes the quantification of I_s to 'S' intervals.

$$I_s = \left\{ \begin{array}{l} \left[-\left(n \left(\frac{\pi - 2K}{s-1} \right) + K \right), -\left((n-1) \left(\frac{\pi - 2K}{s-1} \right) + K \right) \right] \\ \left[-K, K \right] \left[n = 1, \dots, \frac{s-1}{2}, s = 1, 2, \dots, S \right] \\ \left[(n-1) \left(\frac{\pi - 2K}{s-1} \right) + K, n \left(\frac{\pi - 2K}{s-1} \right) + K \right] \end{array} \right\} \quad (2)$$

3.2. Computation of Global Statistics Tri-Directional Pattern (GSTriDP)

Global Statistics Tri Directional Pattern (GSTriDP) is computed for each pixel of an image. Local information from the 3×3 neighborhood of an image and

the global mean [2] value of an image is considered for the computation of GSTriDP. Initially, the sign component of the pattern is constructed. For each surrounding neighbor I_i in the 3×3 neighborhood, the two closest adjacent neighbors are considered as $ad1$ and $ad2$. The intensity differences of each surrounding neighbor with its adjacent neighbors and with the center pixel are calculated using Equation (3).

$$\text{diff}1 = I_i - I_c; \text{diff}2 = I_i - ad1; \text{diff}3 = I_i - ad2 \quad (3)$$

The function in Equation (4) is used to assign the binary value for the sign pattern in each surrounding neighbor.

$$f(I_i) = \begin{cases} 0 & \text{if } _all_diff1, diff2 \& diff3 \leq 0 \text{ or } \geq 0 \\ 1 & \text{otherwise} \end{cases} \quad (4)$$

The Sign Pattern (SP) of the center pixel in the 3×3 neighborhood is mapped using Equation (5).

$$SP(I_c) = \sum_{i=1}^8 f(I_i) \cdot 2^{i-1} \quad (5)$$

The distances between adjacent neighbors of each surrounding pixel with the center pixel and the surrounding pixel are calculated using Equations (6)-(7), respectively.

$$\text{dis}1 = \sqrt{(ad1 - I_c)^2 + (ad2 - I_c)^2} \quad (6)$$

$$\text{dis}2 = \sqrt{(ad1 - I_i)^2 + (ad2 - I_i)^2} \quad (7)$$

Using the function in Equation (8), the binary value for the magnitude pattern in each surrounding neighbor is assigned.

$$g(I_i) = \begin{cases} 1 & \text{if } _dis1 \geq \text{dis}2 \\ 0 & \text{otherwise} \end{cases} \quad (8)$$

The global statistics value is incorporated into the 9th bit of the magnitude pattern. The value of $g(I_9)$ is defined using Equation (9).

$$g(I_9) = \begin{cases} 1 & \text{if } _local_mean \geq \text{global_mean} \\ 0 & \text{otherwise} \end{cases} \quad (9)$$

The Magnitude Pattern (MP) of the center pixel with the inclusion of global statistics in the 3×3 neighborhood is mapped using Equation (10).

$$MP(I_c) = \sum_{i=1}^9 g(I_i) \cdot 2^{i-1} \quad (10)$$

Figure 2 explains how the signed and magnitude components of GSTriDP are computed. The sample 3×3 neighborhood is taken for the calculation. The yellow-colored pixel in the neighborhood is the center pixel. The respective surrounding pixels are colored green. The blue-colored pixels represent the two adjacent neighbors of the corresponding surrounding neighbors. The sign pattern histogram (length of 256(2⁸)) and magnitude pattern histogram (length of 512(2⁹)) are linearly concatenated to form a GSTriDP histogram (length of 768) of an image.

3.3. Image Retrieval Framework Using WGSTriDP

The image retrieval framework for the proposed WGSTriDP is given in Figure 3.

The image retrieval procedure for the proposed methodology is described in Algorithm 1.

Algorithm 1: Image Retrieval using the WGSTriDP Texture feature

Input: Image Database with "n" images, query image (any image from the Image Database), and a criterion(threshold) for defining similarity

Output: Collection of images from the image database that are similar to the query image.

Step 1: Input a query image and an image database to the image retrieval system.

Step 2: Create a 2D WGSTriDP histogram from a query image's differential excitation and GSTriDP histograms.

Step 3: Linearly stretch the 2D WGSTriDP histogram to form the image's feature vector.

Step 4: for i = 1 to n

Step 4.1: Compute the WSGTriDP feature vector of ith image in the Image Database.

Step 4.2: Find the similarity between the query feature vector and the ith image feature vector using similarity function.

Figure 2

Sign and Magnitude patterns computation of GSTriDP in a sample 3×3 neighborhood

Position	Pixels in 3X3 Neighborhood	Working for signed bit(SB) and magnitude bit(MB)									
I ₁	<table border="1"><tr><td>176</td><td>177</td><td>173</td></tr><tr><td>176</td><td>171</td><td>168</td></tr><tr><td>175</td><td>166</td><td>164</td></tr></table>	176	177	173	176	171	168	175	166	164	$\left. \begin{array}{l} \text{diff1}=176-171=5 \\ \text{diff2}=176-176=0 \\ \text{diff3}=176-171=5 \end{array} \right\} 1 \text{ (SB)}$ $\left. \begin{array}{l} \text{dis1}=\sqrt{(176-171)^2+(177-171)^2}=7.8 \\ \text{dis2}=\sqrt{(176-176)^2+(177-176)^2}=1 \end{array} \right\} 1 \text{ (MB)}$
176	177	173									
176	171	168									
175	166	164									
I ₂	<table border="1"><tr><td>176</td><td>177</td><td>173</td></tr><tr><td>176</td><td>171</td><td>168</td></tr><tr><td>175</td><td>166</td><td>164</td></tr></table>	176	177	173	176	171	168	175	166	164	$\left. \begin{array}{l} \text{diff1}=177-171=6 \\ \text{diff2}=177-176=1 \\ \text{diff3}=177-173=4 \end{array} \right\} 0 \text{ (SB)}$ $\left. \begin{array}{l} \text{dis1}=\sqrt{(176-171)^2+(173-171)^2}=5.3 \\ \text{dis2}=\sqrt{(176-177)^2+(173-177)^2}=4.1 \end{array} \right\} 1 \text{ (MB)}$
176	177	173									
176	171	168									
175	166	164									
I ₃	<table border="1"><tr><td>176</td><td>177</td><td>173</td></tr><tr><td>176</td><td>171</td><td>168</td></tr><tr><td>175</td><td>166</td><td>164</td></tr></table>	176	177	173	176	171	168	175	166	164	$\left. \begin{array}{l} \text{diff1}=173-171=2 \\ \text{diff2}=173-177=-4 \\ \text{diff3}=173-168=5 \end{array} \right\} 1 \text{ (SB)}$ $\left. \begin{array}{l} \text{dis1}=\sqrt{(177-171)^2+(168-171)^2}=6.7 \\ \text{dis2}=\sqrt{(177-173)^2+(168-173)^2}=6.4 \end{array} \right\} 1 \text{ (MB)}$
176	177	173									
176	171	168									
175	166	164									
I ₄	<table border="1"><tr><td>176</td><td>177</td><td>173</td></tr><tr><td>176</td><td>171</td><td>168</td></tr><tr><td>175</td><td>166</td><td>164</td></tr></table>	176	177	173	176	171	168	175	166	164	$\left. \begin{array}{l} \text{diff1}=168-171=-3 \\ \text{diff2}=168-173=-5 \\ \text{diff3}=168-164=4 \end{array} \right\} 1 \text{ (SB)}$ $\left. \begin{array}{l} \text{dis1}=\sqrt{(173-171)^2+(164-171)^2}=7.2 \\ \text{dis2}=\sqrt{(173-168)^2+(164-168)^2}=6.4 \end{array} \right\} 1 \text{ (MB)}$
176	177	173									
176	171	168									
175	166	164									
I ₅	<table border="1"><tr><td>176</td><td>177</td><td>173</td></tr><tr><td>176</td><td>171</td><td>168</td></tr><tr><td>175</td><td>166</td><td>164</td></tr></table>	176	177	173	176	171	168	175	166	164	$\left. \begin{array}{l} \text{diff1}=164-171=-7 \\ \text{diff2}=164-168=-4 \\ \text{diff3}=164-166=-2 \end{array} \right\} 0 \text{ (SB)}$ $\left. \begin{array}{l} \text{dis1}=\sqrt{(168-171)^2+(166-171)^2}=5.8 \\ \text{dis2}=\sqrt{(168-164)^2+(166-164)^2}=4.4 \end{array} \right\} 1 \text{ (MB)}$
176	177	173									
176	171	168									
175	166	164									
I ₆	<table border="1"><tr><td>176</td><td>177</td><td>173</td></tr><tr><td>176</td><td>171</td><td>168</td></tr><tr><td>175</td><td>166</td><td>164</td></tr></table>	176	177	173	176	171	168	175	166	164	$\left. \begin{array}{l} \text{diff1}=166-171=-5 \\ \text{diff2}=166-164=2 \\ \text{diff3}=166-175=-9 \end{array} \right\} 1 \text{ (SB)}$ $\left. \begin{array}{l} \text{dis1}=\sqrt{(164-171)^2+(175-171)^2}=8.1 \\ \text{dis2}=\sqrt{(164-166)^2+(175-166)^2}=9.2 \end{array} \right\} 0 \text{ (MB)}$
176	177	173									
176	171	168									
175	166	164									
I ₇	<table border="1"><tr><td>176</td><td>177</td><td>173</td></tr><tr><td>176</td><td>171</td><td>168</td></tr><tr><td>175</td><td>166</td><td>164</td></tr></table>	176	177	173	176	171	168	175	166	164	$\left. \begin{array}{l} \text{diff1}=175-171=4 \\ \text{diff2}=175-166=9 \\ \text{diff3}=175-176=-1 \end{array} \right\} 1 \text{ (SB)}$ $\left. \begin{array}{l} \text{dis1}=\sqrt{(166-171)^2+(176-171)^2}=7.1 \\ \text{dis2}=\sqrt{(166-175)^2+(176-175)^2}=9.1 \end{array} \right\} 0 \text{ (MB)}$
176	177	173									
176	171	168									
175	166	164									
I ₈	<table border="1"><tr><td>176</td><td>177</td><td>173</td></tr><tr><td>176</td><td>171</td><td>168</td></tr><tr><td>175</td><td>166</td><td>164</td></tr></table>	176	177	173	176	171	168	175	166	164	$\left. \begin{array}{l} \text{diff1}=176-171=5 \\ \text{diff2}=176-175=1 \\ \text{diff3}=176-176=0 \end{array} \right\} 0 \text{ (SB)}$ $\left. \begin{array}{l} \text{dis1}=\sqrt{(175-171)^2+(176-171)^2}=6.4 \\ \text{dis2}=\sqrt{(175-176)^2+(176-176)^2}=1 \end{array} \right\} 1 \text{ (MB)}$
176	177	173									
176	171	168									
175	166	164									
Signed Pattern : 01101101											
Magnitude Pattern : X10011111 [X may be '0' or '1' depending upon the relation between the local mean and global mean]											

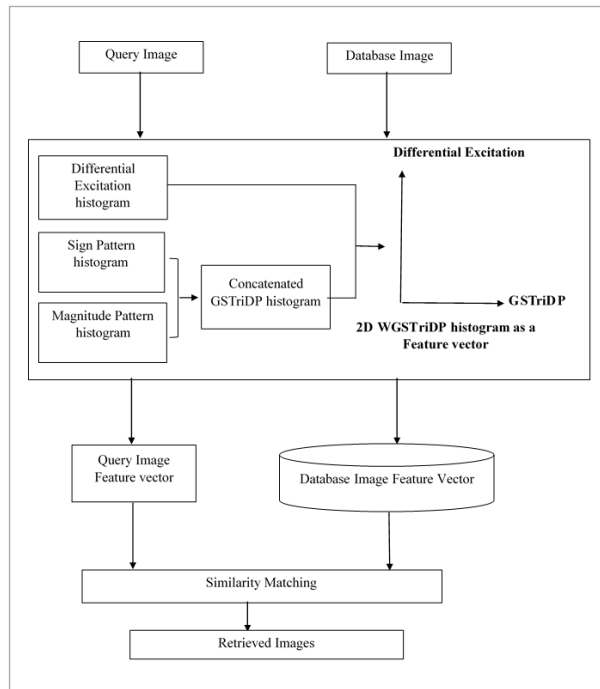
Step 4.3: If the similarity value is less than the threshold, store the image in the image database as the relevant images to the search query

Step 5: Show all of the query image's relevant images.

The similarity measure also contributes to the result of image retrieval. This process uses the distance metric to find the similarity between the database image feature vector and the query image feature vector. Several distance metrics are used to find the similarity between a query image and the database image. The d1 distance measure is an excellent distance measure for local patterns among the various distance metrics [20,21,37]. The d1 distance measure is given in Equation (11).

$$d1(x, y) = \sum_{i=0}^{n-1} \left| \frac{x_i - y_i}{1 + x_i + y_i} \right| \quad (11)$$

Figure 3
Proposed Image Retrieval Framework using WGSTriDP
Texture Descriptor



The values 'x' and 'y' in Equation (11) represent the feature vector of the database image and query image, respectively. The value 'n' represents the length of the feature vector.

4. Experimental Results and Discussions

This work proposes the Weber Global Statistics Tri-directional Pattern (WGSTriDP) for image retrieval. The performance of the pattern in image retrieval is tested in two benchmark databases, known as the ORL database and the UIUC database. The ORL database consists of 40 classes of face images. Each class consists of 10 images, and 400 images in total. The UIUC database consists of 25 classes of gray texture images. Each class has 40 images, thereby, it has 1000 images in the database. Sample images of the ORL database and the UIUC database are given in Figures 4-5, respectively.

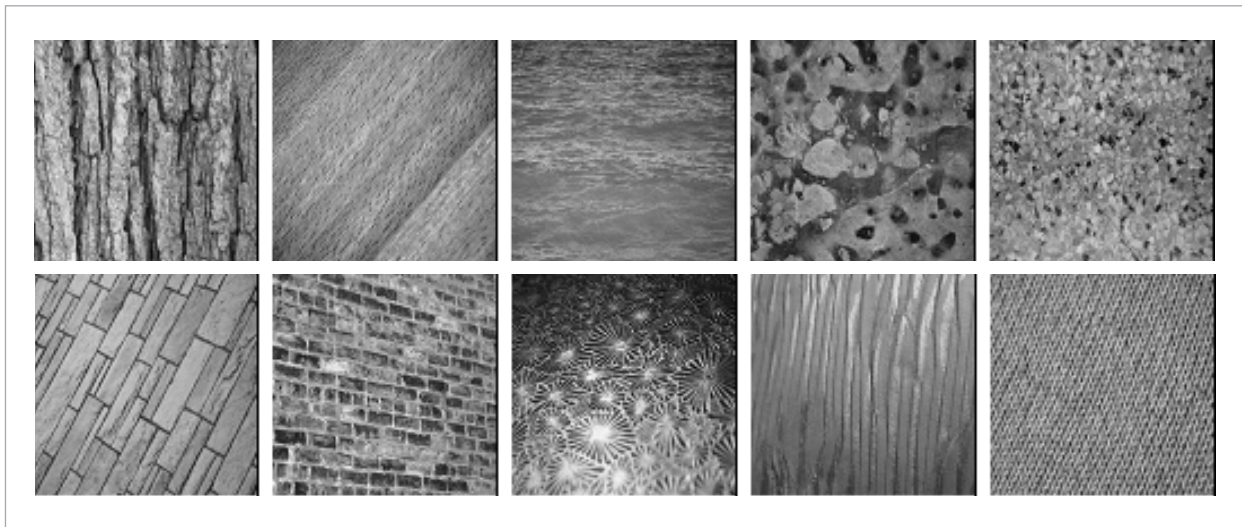
Initially, all the images in the database are converted into the WGSTriDP feature vector. Each image in the database takes the role of the query image to retrieve similar images from the database. The top 'n' number of relevant images are retrieved as the result. The different values of 'n' can be taken for experiments. The performance of the proposed

Figure 4
Sample Images of ORL Database



Figure 5

Sample Images of the UIUC Database



retrieval algorithm is measured by precision and recall measures [19] and they are given in Equations (12)-(13), respectively.

$$\text{Precision} = \frac{\text{Number_of_Relevant_Images_Retrieved}}{\text{Total_Number_of_Images_Retrieved}} \quad (12)$$

$$\text{Recall} = \frac{\text{Number_of_Relevant_Images_Retrieved}}{\text{Total_Number_of_Relevant_Images_in_the_Database}} \quad (13)$$

Four experiments were carried out for the proposed method. The construction of the WSGTriDP feature vector involves the formation of a differential excitation histogram. Many differential excitation histograms can be formed for the same image concerning values of 'K' and 'S' as given in Equation (2). Experiment 1 of the work tests the effectiveness of the WSGTriDP feature in the ORL database for the values of K=30,45,60 and S=3,5,7. Experiment 2 analyses the performance of WSGTriDP against LTriDP, LNIP, and LBP. Experiment 3 observes the performance of WSGTriDP against the LTriDP and LNIP with the incorporation of differential excitation components. They are called Weber LTriDP (WLTriDP) and Weber LNIP (WLNIP). Experiment 4 tests the robustness of the proposed feature.

4.1. Experiment 1

The ORL database is considered for this experiment. The purpose of this experiment is to reduce the complexity of constructing the WSGTriDP feature vector by trimming down the complexity involving the formation of differential excitation components. The complexity of forming differential excitation can be reduced by fixing the high perception range(K) and intervals(S). The performance of the image retrieval with WSGTriDP is analyzed with various K=30,45,60 and S=3,5,7 to find the optimal value of K and S. The precision comparison of WSGTriDP based ORL database image retrieval system for different values of 'K' and 'S' in the differential excitation component is given in the Table 1.

It is inferred from Table 1 that, the precision values of K=30, S=5, and K=30, S=7 are superior to other ranges and intervals. As the 'K' value decreases, the range of high perception intervals is wider. The high perception interval contains more information, hence the K=30 range gives the best precision values. The K=30, S=7 WSGTriDP histogram is lengthier than the K=30, S=5 histogram. It is decided to use K=30 and S=5 in the computation of differential excitation components for further experiments.

Table 1

Precision Comparison of WGSTriDP based ORL database image retrieval system with different K and S

Number of Top Images Retrieved	K=60,S=3	K=60,S=5	K=60,S=7	K=45,S=3	K=45,S=5	K=45,S=7	K=30,S=3	K=30,S=5	K=30,S=7
1	1	1	1	1	1	1	1	1	1
2	0.94	0.94	0.94	0.96	0.96	0.96	0.96	0.97	0.97
3	0.89	0.89	0.89	0.9	0.91	0.9	0.94	0.94	0.94
4	0.86	0.86	0.86	0.89	0.89	0.89	0.9	0.9	0.9
5	0.84	0.84	0.83	0.86	0.86	0.86	0.86	0.86	0.86
6	0.8	0.8	0.8	0.8	0.8	0.8	0.8	0.8	0.8
7	0.71	0.71	0.71	0.73	0.73	0.73	0.75	0.75	0.75
8	0.67	0.67	0.67	0.68	0.68	0.68	0.71	0.71	0.71
9	0.64	0.64	0.64	0.66	0.66	0.66	0.66	0.66	0.66
10	0.63	0.63	0.63	0.63	0.63	0.63	0.63	0.63	0.63

4.2. Experiment 2

The performance of WGSTriDP in terms of precision and recall is analyzed against the LTriDP, LNIP, and LBP in this experiment. The LTriDP and LNIP are considered because they also derive sign and magnitude patterns from the neighborhood. All the images in the ORL database (400 images) and UIUC database (1000 images) are passed as a query to derive the average precision and average recall values. The ORL database image retrieval system analyses the precision and recall values from the Top 1 images retrieved to the Top 10 images retrieved in the interval of 1. The UIUC database image retrieval system analyses the precision values from Top 1 images retrieved to Top 10 images retrieved in the interval of 1 and precision and recall values from Top 4 images retrieved to Top 40 images retrieved in the interval of 4.

Precision and recall comparison of the ORL based image retrieval system for the Top 1 images retrieved to the Top 10 images retrieved in the interval of 1 is given in Figures 6-7, respectively.

From the average precision values of WGSTriDP (0.82), LTriDP (0.63), LNIP (0.56), and LBP (0.52) for Top 1 images retrieved to Top 10 images retrieved in the ORL database image retrieval system, it is clear that the proposed WGSTriDP has an increase of 19% from LTriDP, a 26% increase from LNIP, and a 30% increase from LBP in average precision values.

A precision comparison of UIUC based image retrieval system for Top 1 images retrieved to Top 10 images retrieved in the interval of 1 is given in Figure 8.

From the average precision values of WGSTriDP (0.75), LTriDP (0.64), LNIP (0.64), and LBP (0.61) for the Top 1 images retrieved to the Top 10 images retrieved in the UIUC database image retrieval system, it is clear that the proposed WGSTriDP has an increase of 11% from LTriDP, an 11% increase from LNIP and, a 14% increase from LBP in average precision values.

Figure 6

Precision comparison of WGSTriDP, LTriDP, LNIP, and LBP based image retrieval systems in the ORL database for Top 10 images retrieved

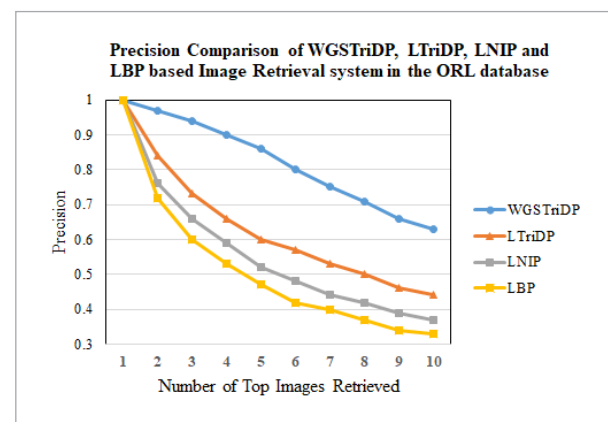


Figure 7

Recall comparison of WGSTriDP, LTriDP, LNIP, and LBP based image retrieval systems in the ORL database for Top 10 images retrieved

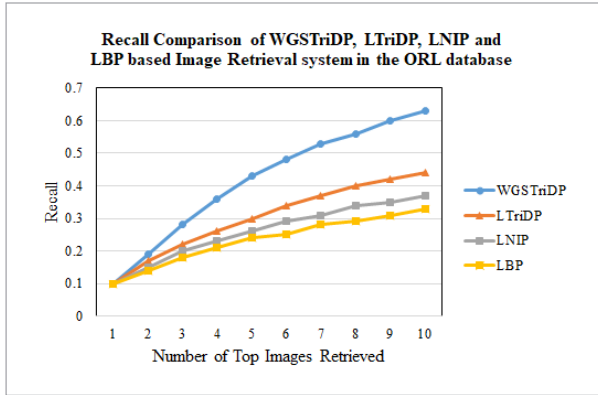


Figure 9

Precision comparison of WGSTriDP, LTriDP, LNIP, and LBP based image retrieval systems in the UIUC database for Top 40 images retrieved

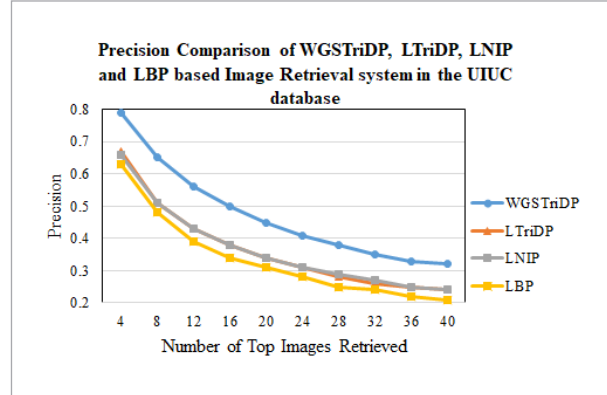


Figure 8

Precision comparison of WGSTriDP, LTriDP, LNIP, and LBP based image retrieval systems in the UIUC database for Top 10 images retrieved

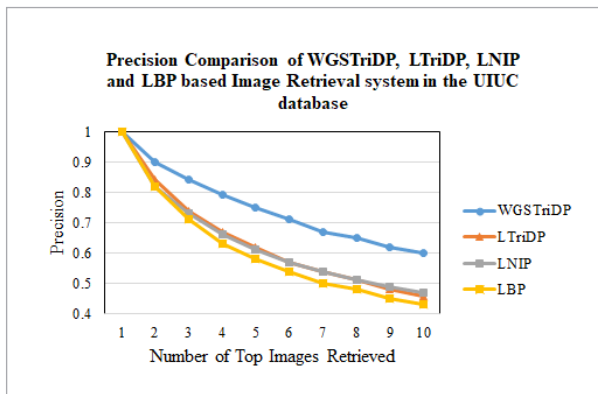
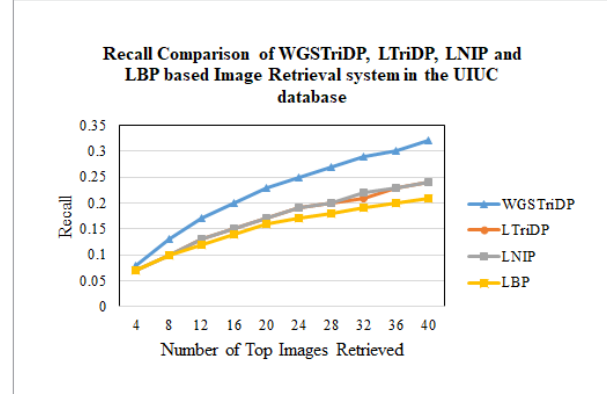


Figure 10

Recall comparison of WGSTriDP, LTriDP, LNIP, and LBP based image retrieval systems in the UIUC database for Top 40 images retrieved



Precision and recall comparisons of the UIUC based image retrieval system for the Top 4 images retrieved to the Top 40 images retrieved in the interval of 4 are given in Figures 9-10, respectively.

It is observed from Figures 6-10 and the average precision analysis of the Top 1 to Top 10 images retrieved, that the WGSTriDP based image retrieval framework performed well as compared to LTriDP, LNIP, and LBP based image retrieval frameworks.

4.3. Experiment 3

Experiment 3 is conducted to verify the influence of differential excitation components in LTriDP and

LNIP feature descriptors. The new texture feature descriptors Weber LTriDP (WLTriDP) and Weber LNIP (WLNIP) are formed. WLTriDP is formed from differential excitation and LTriDP components. WLNIP is formed from differential excitation and LNIP components. The efficacy of the WGSTriDP based image retrieval system is compared with that of the WLTriDP and WLNIP based image retrieval systems. Precision and recall values of the ORL based image retrieval system for WGSTriDP, WLTriDP, and WLNIP for Top 1 images retrieved to Top 10 images retrieved in the interval of 1, are given in Figures 11-12, respectively.

Figure 11

Precision comparison of WGSTriDP, WLTriDP, and WLNIP based image retrieval systems in the ORL database for Top 10 images retrieved

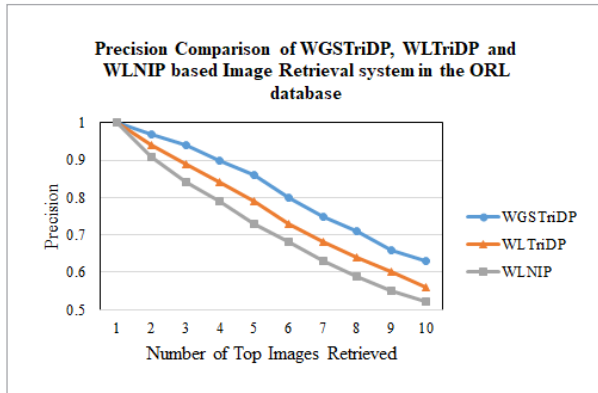
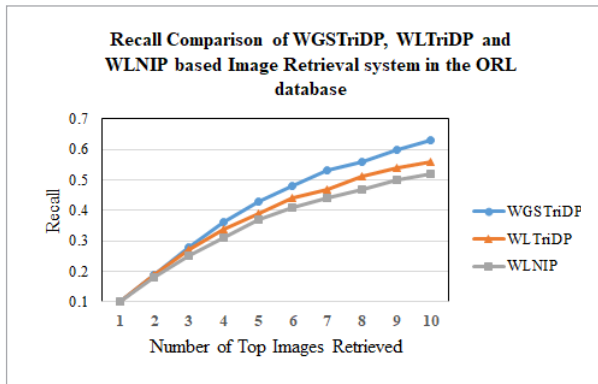


Figure 12

Recall comparison of WGSTriDP, WLTriDP, and WLNIP based image retrieval systems in the ORL database for Top 10 images retrieved



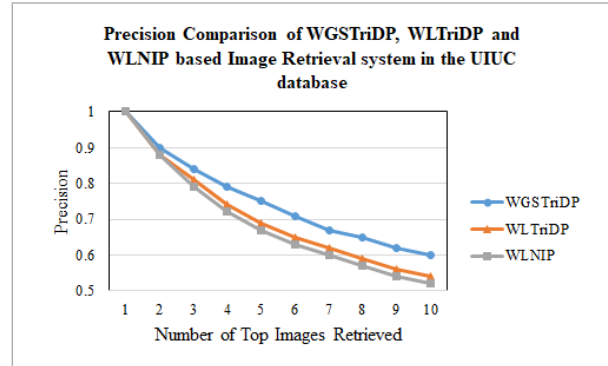
From the average precision values of WGSTriDP (0.82), WLTriDP (0.77), and WLNIP (0.72) for the Top 1 images retrieved to the Top 10 images retrieved in the ORL database image retrieval system, it is clear that the proposed WGSTriDP has an increase of 5% from WLTriDP and a 10% increase from WLNIP in average precision values.

Precision comparisons of UIUC based image retrieval system for WGSTriDP, WLTriDP, and WLNIP for Top 1 images retrieved to Top 10 images retrieved in the interval of 1 is given in Figure 13.

From the average precision values of WGSTriDP (0.75), WLTriDP (0.71), and WLNIP (0.69) for the Top 1 images retrieved to the Top 10 images retrieved in

Figure 13

Precision comparison of WGSTriDP, WLTriDP, and WLNIP based image retrieval systems in the UIUC database for Top 10 images retrieved



the UIUC database image retrieval system, it is clear that the proposed WGSTriDP has an increase of 4% from WLTriDP and a 6% increase from WLNIP in average precision values.

Precision and recall comparisons of UIUC based image retrieval system for the Top 4 images retrieved to the Top 40 images retrieved in the interval of 4 are given in Figures 14-15, respectively.

It is observed from Figures 11-15 and the average precision analysis of the Top 1 to Top 10 images retrieved, that the WGSTriDP based image retrieval framework performed superior to WLTriDP and WLNIP. The experimental results show that the superiority of WGSTriDP not only depends on the differential excitation component, but also on three factors. They are

Figure 14

Precision comparison of WGSTriDP, WLTriDP, and WLNIP based image retrieval systems in the UIUC database for Top 40 images retrieved

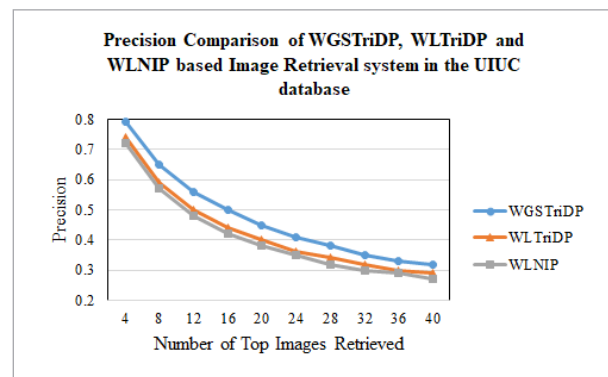
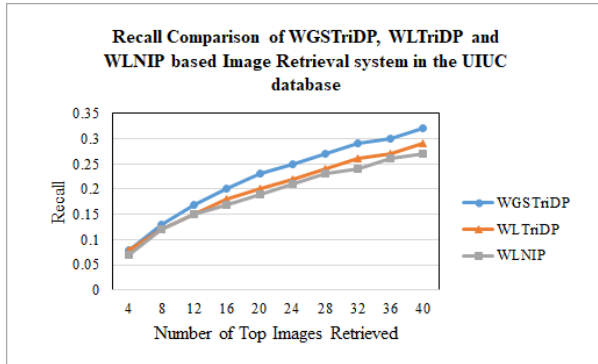


Figure 15

Recall comparison of WGSTriDP, WLTriDP, and WLNIIP based image retrieval systems in the UIUC database for Top 40 images retrieved



the differential excitation component, the encoding of sign and magnitude components in the neighborhood, and the inclusion of global statistics.

4.4. Experiment 4

Experiment 4 is conducted to uphold the robustness of the WGSTriDP feature in the presence of salt and pepper noise. Image retrieval is performed after adding salt and pepper noise to the ORL and UIUC images. The salt and pepper noise was chosen because it does not completely affect the image; rather, it affects only some of the pixels in the image. In the neighborhood, there is a possibility that some neighbors are not affected [9]. Since the proposed descriptor and other descriptors which are taken for the experiments are neighborhood relation oriented, the inclusion of salt and pepper noise in the images is chosen to experiment with the robustness of such descriptors. Figure 16 illustrates the average precision comparison of the ORL based image retrieval system in the presence of salt and pepper noise.

The precision values of the WGSTriDP based ORL image retrieval system are comparatively high as opposed to others in the presence of 10% of noise (75%), 20% of noise (71%), 30% of noise (66%), and 40% of noise (63%).

Figure 17 depicts the average precision comparison of the UIUC based image retrieval system in the presence of salt and pepper noise.

The precision values of the WGSTriDP based UIUC image retrieval system are relatively high as com-

Figure 16

Average Precision comparison of WGSTriDP, WLTriDP, WLNIIP, LTriDP, LNIP, and LBP based image retrieval systems in the ORL database for Top 1 to Top 10 images retrieved

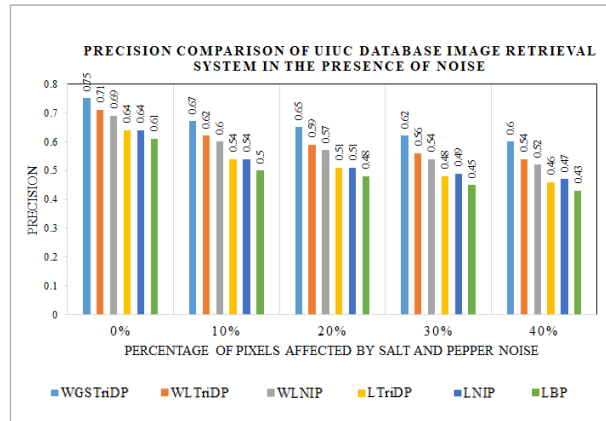
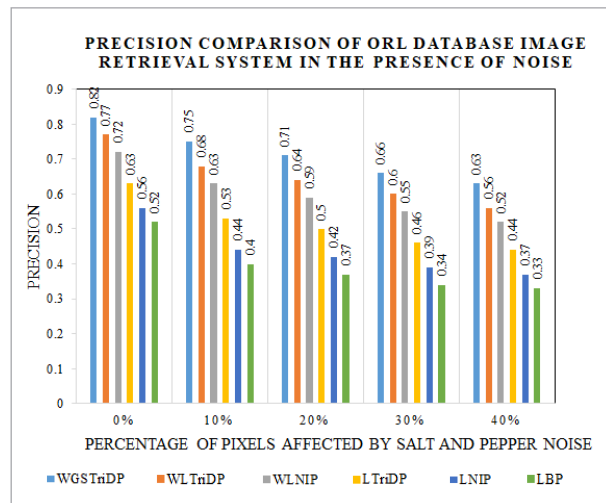


Figure 17

Average Precision comparison of WGSTriDP, WLTriDP, WLNIIP, LTriDP, LNIP, and LBP based image retrieval systems in the UIUC database for Top 1 to Top 10 images retrieved



pared to others in the presence of 10% of noise (67%), 20% of noise (65%), 30% of noise (62%), and 40% of noise (60%).

It is perceived from Figures 16-17 that, the WGSTriDP is performing well even in the presence of noise as compared to other descriptors that are considered. The performance of the WGSTriDP based image retrieval is compared with others in the presence of up

to 40% of the noise, since the degradation of the image is greater when a greater amount of noise is included. The experimental results from experiment 4.2 to experiment 4.4 reveal that WGSTriDP based image retrieval system outperforms the other contemporary texture descriptors in both ORL and UIUC databases even in the presence of noise.

5. Conclusion

The most successful texture descriptor, called Weber Global Statistics Tri-Directional Pattern (WGSTriDP) for image retrieval is presented in this article. The WGSTriDP effectively combines the dif-

ferential excitation component from WLD, the sign and magnitude components from the local neighborhood in a circular fashion, and the global statistics of an image. The proposed descriptor is tested over the ORL and UIUC databases for image retrieval applications. The effectiveness of the proposed method is compared with existing standard texture descriptors with the help of precision and recall values. The robustness of the proposed method is tested with the presence of salt and pepper noise. The results proved that the Weber Global Statistics Tri-Directional Pattern outstrips other descriptors in all aspects. It is recommended that Weber Global Statistics Tri-Directional Pattern (WGSTriDP) be used as a texture representation for any image processing applications.

References

- Banerjee, P., Bhunia, A. K., Bhattacharyya, A., Roy, P. P., Murala, S. Local Neighborhood Intensity Pattern-A New Texture Feature Descriptor for Image Retrieval. *Experts Systems with Applications*, 2018, 113, 100-115. <https://doi.org/10.1016/j.eswa.2018.06.044>
- Callinschriyana, C., Rajamani, V. Global Neighbour Preserving Local Ternary Co-occurrence Pattern (GN-PLTCoP) for Ultrasound Kidney Images Retrieval. *Indian Journal of Science and Technology*, 2015, 8(7), 614-621. <https://doi.org/10.17485/ijst/2015/v8i7/62845>
- Chen, J., Shan, S., He, C., Zhao, G., Pietikainen, M., Chen, X., Gao, W. WLD: A Robust Local Image Descriptor. *IEEE Transactions on Pattern Analysis and Machine Intelligence*, 2010, 32(9), 1705-1720. <https://doi.org/10.1109/TPAMI.2009.155>
- Ershad, S. F. Bark Texture Classification Using Improved Local Ternary Patterns and Multilayer Neural Network. *Expert Systems with Applications*, 2020, 158, 113509. <https://doi.org/10.1016/j.eswa.2020.113509>
- Guo, Z., Zhang, L., Zhang, D. A Completed Modeling of Local Binary Pattern Operator for Texture Classification. *IEEE Transactions on Image Processing*, 2010, 19(6), 1657- 1663. <https://doi.org/10.1109/TIP.2010.2044957>
- Haralick, R. M., Shanmugam, K., Dinstein, I. H. Textural features for Image Classification. *IEEE Transactions on Systems, Man, and Cybernetics*, 1973, 3(6), 610-621. <https://doi.org/10.1109/TSMC.1973.4309314>
- Huang, J., Kumar, S. R., Mitra, M., Zhu, W. J., Zabih, R. Image Indexing Using Color Correlograms. *Proceedings of IEEE Computer Society Conference on Computer Vision and Pattern Recognition*, San Juan, PR, USA, Jun 17-19, 1997, 762-768. <https://dl.acm.org/doi/10.5555/794189.794514>
- Huang, Z., Chan, P. P. K., Ng, W. W. Y., Yeung, D. S., Content-based Image Retrieval Using Color Moment and Gabor Texture Feature. *International Conference on Machine Learning and Cybernetics*, Qingdao, China, Jul 11-14, 2010, 719-724. <https://doi.org/10.1109/ICMLC.2010.5580566>
- Joshi, A., Boyat, A. K., Joshi, B. K. Impact of Wavelet Transform and Median Filtering on Removal of Salt and Pepper Noise in Digital Images. *IEEE International Conference on Issues and Challenges in Intelligent Computing Techniques (ICICT)*, Gaziabad, India, Feb 7-8, 2014, 838-843. <https://doi.org/10.1109/ICICT.2014.6781389>
- Kanwal, K., Ahmad, K. T., Khan, R., Alhusaini, N., Jing, L. Deep Learning Using Isotroping, Laplacing, Eigenvalues Interpolative Binding, and Convolved Determinants with Normed Mapping for Large- Scale Image Retrieval. *Sensors*, 2021, 21(4), 1139. <https://doi.org/10.3390/s21041139>
- Kanwal, K., Ahmad, K. T., Khan, R., Abbasi, A. T., Li, J. Deep Learning Using Symmetry, FAST Scores, Shape-Based Filtering and Spatial Mapping Integrated with CNN for Large Scale Image Retrieval. *Symmetry*, 2020, 12(4), 612. <https://doi.org/10.3390/sym12040612>
- Kas, M., Khadiri, I. E., Merabet, Y. E., Ruichek, Y., Messoussi, R. Multi Level Directional Cross Binary Pat-

- terms: New Handcrafted Descriptor for SVM- based Texture Classification. *Engineering Applications of Artificial Intelligence*, 2020, 94, 103743. <https://doi.org/10.1016/j.engappai.2020.103743>
13. Kekre, H. B., Thepade, S. D., Lohar, A. T. Image Retrieval Using Block Truncation Coding Extended to Color Clumps. *Proceedings of the 2013 International Conference on Advances in Technology and Engineering*, Mumbai, India, Jan 23-25, 2013, 1-6. <https://doi.org/10.1109/ICAdTE.2013.6524769>
 14. Liao, S., Law, M. W. K., Chung, A. C. S. Dominant Local Binary Patterns for Texture Classification. *IEEE Transactions on Image Processing*, 2009, 18(5), 1107-1118. <https://doi.org/10.1109/TIP.2009.2015682>
 15. Liu, F., Tang, Z., Tang, J. WLBP: Weber Local Binary Pattern for Local Image Description. *Neurocomputing*, 2013, 120, 325-335. <https://doi.org/10.1016/j.neucom.2012.06.061>
 16. Liu, Y., Zhang, D., Lu, G., Ma, W. Y. A Survey of Content-based Image Retrieval with High-level Semantics. *Pattern Recognition*, 2007, 40 (1), 262- 282. <https://doi.org/10.1016/j.patcog.2006.04.045>
 17. Loupias, E., Sebe, N., Bres, S., Jolion, J. M. Wavelet-based Salient Points for Image Retrieval. *Proceedings of IEEE 7th International Conference on Image Processing*, Vancouver, BC, Canada, Sep 10-13, 2000, 518-521. <https://doi.org/10.1109/ICIP.2000.899469>
 18. Manjunath, B. S., Ma, W. Y. Texture Features for Browsing and Retrieval of Image Data. *IEEE Transactions on Pattern Analysis and Machine Intelligence*, 1996, 18(8), 837-842. <https://doi.org/10.1109/34.531803>
 19. Muller, H., Muller, W., Squire, D. M., Maillet, S. M., Pun, T. Performance Evaluation in Content-based Image Retrieval: Overview and Proposals. *Pattern Recognition Letters*, 2001, 22(5), 593-601. [https://doi.org/10.1016/S0167-8655\(00\)00118-5](https://doi.org/10.1016/S0167-8655(00)00118-5)
 20. Murala, S., Maheshwari, R. P., Balasubramanian, R. Directional Local Extrema Patterns: A New Descriptor for Content Based Image Retrieval. *International Journal of Multimedia Information Retrieval*, 2012, 1, 191-203. <https://doi.org/10.1007/s13735-012-0008-2>
 21. Murala, S., Maheshwari, R. P., Balasubramanian, R. Local Tetra Patterns: A New Feature Descriptor for Content- Based Image Retrieval. *IEEE Transactions on Image Processing*, 2012, 21(5), 2874-2886. <https://doi.org/10.1109/TIP.2012.2188809>
 22. Murala, S., Maheshwari, R. P., Balasubramanian, R. Local Maximum Edge Binary Patterns: A New Descriptor for Image Retrieval and Object Tracking. *Signal Processing*, 2012, 92(6), 1467-1479. <https://doi.org/10.1016/j.sigpro.2011.12.005>
 23. Murala, S., Wu, Q. M. J. Local Ternary Co-occurrence Patterns: A New Feature Descriptor for MRI and CT Image Retrieval. *Neurocomputing*, 2013, 119, 399-412. <https://doi.org/10.1016/j.neucom.2013.03.018>
 24. Ojala, T., Pietikainen, M., Harwood, D. A Comparative Study of Texture Measures with Classification Based on Featured Distributions. *Pattern Recognition*, 1996, 29(1), 51-59. [https://doi.org/10.1016/0031-3203\(95\)00067-4](https://doi.org/10.1016/0031-3203(95)00067-4)
 25. Ojala, T., Pietikainen, M., Maenpaa, T. Multiresolution Gray-scale and Rotation Invariant Texture Classification with Local Binary Patterns. *IEEE Transactions on Pattern Analysis and Machine Intelligence*, 2002, 24(7), 971-987. <https://doi.org/10.1109/TPAMI.2002.1017623>
 26. Pass, G., Zabih, R., Miller, J. Comparing Images Using Color Coherence Vectors. *Proceedings of the Fourth ACM International Conference on Multimedia*, Boston Massachusetts, USA, Nov 18-22, 1996, 65-73. <https://doi.org/10.1145/244130.244148>
 27. Shao, H., Wu, Y., Cui, W., Zhang, J. Image Retrieval Based on MPEG-7 Dominant Color Descriptor. *Proceedings of the 9th International Conference for Young Computer Scientists*, Hunan, China, Nov 18-21, 2008, 753-757. <https://doi.org/10.1109/ICYCS.2008.89>
 28. Shinde, P., Sinkar, A., Tora, M., Halhalli, S. Image Retrieval Based on its Contents Using Features Extraction. *International Research Journal of Engineering and Technology*, 2016, 3(1), 505-509.
 29. Shu, X., Song, Z., Shi, J., Huang, S., Wu, X. J. Multiple Channels Local Binary Pattern for Color Texture Representation and Classification. *Signal Processing: Image Communication*, 2021, 98, 116392. <https://doi.org/10.1016/j.image.2021.116392>
 30. Sukhia, K. N., Riaz, M. M., Ghafoor, A., Ali, S. S. Content-based Remote Sensing Image Retrieval Using Multi-scale Local Ternary Pattern. *Digital Signal Processing*, 2020, 104, 102765. <https://doi.org/10.1016/j.dsp.2020.102765>
 31. Sukhia, K. N., Riaz, M. M., Ghafoor, A., Ali, S. S., Iltaf, N. Content-based Histopathological Image Retrieval Using Multi-scale and Multichannel Decoder based LTP. *Biomedical Signal Processing and Control*, 2019, 54, 101582. <https://doi.org/10.1016/j.bspc.2019.101582>
 32. Sumana, I. J., Islam, M. M., Zhang, D., Lu, G. Content Based Image Retrieval Using Curvelet Transform. *Pro-*

- ceedings of the IEEE 10th Workshop on Multimedia Signal Processing, Cairns, QLD, Australia, Oct 8-10, 2008, 11-16. <https://doi.org/10.1109/MMSP.2008.4665041>
33. Tamura, H., Mori, S., Yamawaki, T. Textural Features Corresponding to Visual Perception. *IEEE Transactions on Systems, Man, and Cybernetics*, 1978, 8(6), 460-473. <https://doi.org/10.1109/TSMC.1978.4309999>
34. Tan, X., Triggs, B. Enhanced Local Texture Feature Sets for Face Recognition Under Difficult Lighting Conditions. *IEEE Transactions on Image Processing*, 2010, 19 (6), 1635-1650. <https://doi.org/10.1109/TIP.2010.2042645>
35. Tian, D. P. A Review on Image Feature Extraction and Representation Techniques. *International Journal of Multimedia and Ubiquitous Engineering*, 2013, 8(4), 385-396.
36. Verma, M., Balasubramanian, R. Local Neighborhood Difference Pattern: A New Feature Descriptor for Natural and Texture Image Retrieval. *Multimedia Tools and Applications*, 2018, 77, 11843-11866. <https://doi.org/10.1007/s11042-017-4834-3>
37. Verma, M., Balasubramanian, R. Center Symmetric Local Binary Co-occurrence Pattern for Texture, Face and Bio-medical Image Retrieval. *Journal of Visual Communication and Image Representation*, 2015, 32, 224-236. <https://doi.org/10.1016/j.jvcir.2015.08.015>
38. Verma, M., Balasubramanian, R. Local Tri-directional Patterns: A New Texture Feature Descriptor for Image Retrieval. *Digital Signal Processing*, 2016, 51, 62-72. <https://doi.org/10.1016/j.dsp.2016.02.002>
39. Wang, X. Y., Wu, J. F., Yang, H. Y. Robust Image Retrieval Based on Color Histogram of Local Feature Regions. *Multimedia Tools and Applications*, 2010, 49, 323-345. <https://doi.org/10.1007/s11042-009-0362-0>
40. Zhang, D., Islam, M. M., Lu, G. A Review on Automatic Image Annotation Techniques. *Pattern Recognition*, 2012, 45(1), 346-362. <https://doi.org/10.1016/j.patcog.2011.05.013>
41. Zhang, B., Gao, Y., Zhao, S., Liu, J. Local Derivative Pattern Versus Local Binary Pattern: Face Recognition With High-Order Local Pattern Descriptor. *IEEE Transactions on Image Processing*, 2010, 19(2), 533-544. <https://doi.org/10.1109/TIP.2009.2035882>
42. Zhang, D., Lu, G. Review of Shape Representation and Description Techniques. *Pattern Recognition*, 2004, 37(1), 1-19. <https://doi.org/10.1016/j.patcog.2003.07.008>

